AD-A049 827 BROWN UNIV PROVIDENCE R I DIV OF ENGINEERING F/G 20/11
FINITE VISCOPLASTIC DEFLECTIONS OF AN IMPULSIVELY LOADED PLATE --ETC(U)
SEP 77 P S SYMONDS, C T CHON N00014-75-C-0860
UNCLASSIFIED N00014-0860/5 NL

1 of 1
ADA049 827

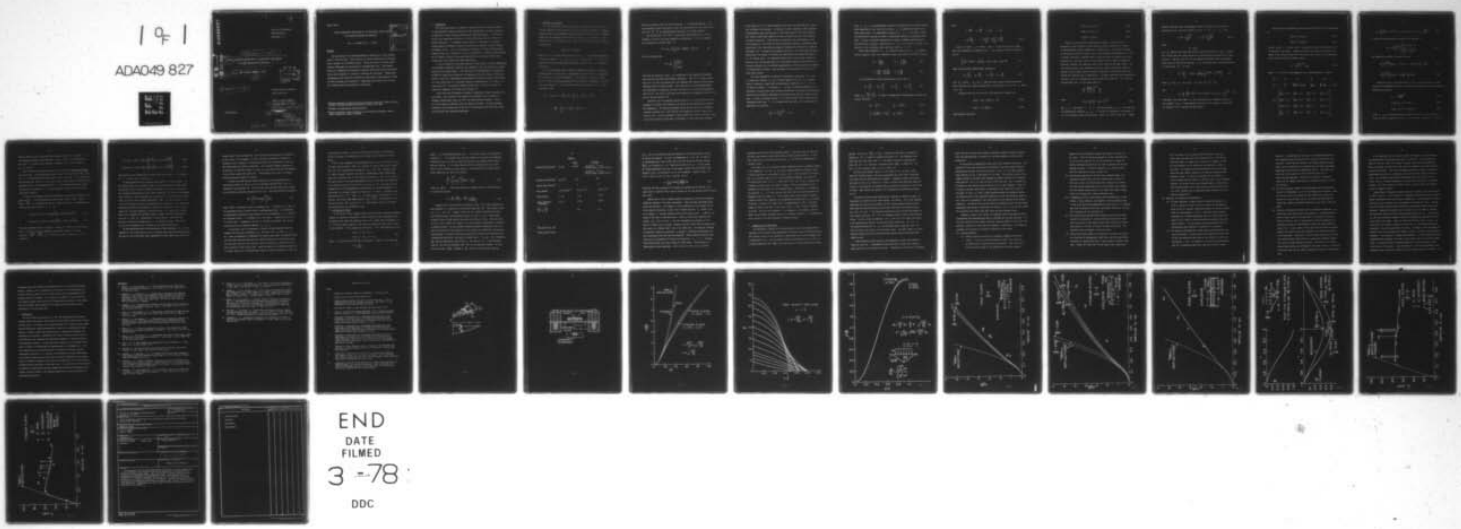

END
DATE FILMED
3-78
DDC

Division of Engineering

BROWN UNIVERSITY

PROVIDENCE, R. I.

(9) Technical rept.,

(6) FINITE VISCOPLASTIC DEFLECTIONS OF AN IMPULSIVELY LOADED PLATE BY THE MODE APPROXIMATION TECHNIQUE.

(10) Paul S. Symonds and T. Chon

Choon

(14) N00014-0860/5

National Science Foundation

Grant ENG74-21258

Office of Naval Research

(15) Contract N00014-75-C-0860,

NSF-Eng-74-21258

N00014 0860/5

(11) Sep[redacted]977

(12) 42 p.

065 310

1473

N00014 0860/5

FINITE VISCOPLASTIC DEFLECTIONS OF AN IMPULSIVELY LOADED PLATE BY THE MODE APPROXIMATION TECHNIQUE[1]

by P. S. Symonds[2] and C. T. Chon[3]

Abstract

The application of the mode approximation technique to a fully clamped plate is here described. Mode solutions for finite deflections are obtained from a sequence of instantaneous modes. Master solutions for chosen initial velocity amplitudes are constructed in nondimensional form. These depend weakly on a parameter of viscoplastic material behavior and size of structure, and so can be applied to a variety of loadings and structures. Finding each instantaneous mode shape and acceleration constitutes an eigen-problem, solved by finite elements with iterations. Comparisons with recent tests on steel and titanium plates are discussed in some detail.

[1]Research supported by National Science Foundation under Grant ENG74-21258 and by Office of Naval Research under Contract N00014-75-C-0860.

[2]Professor of Engineering, Brown University.

[3]Research Associate, Brown University; now at Research Laboratory, General Motors Corporation, Warren, Michigan.

1. Introduction

The "mode approximation" technique, suggested first for impulsive loading of rigid-perfectly plastic structures at small deflections [1], must be modified if conditions of many practical problems are taken into account. In particular, plastic rate dependence and effects of large deflections make the original approach unrealistic. The clamped circular plate is a case where the behavior becomes markedly different as finite deflections are reached, flexural changing to membrane action. Due to the increase in stiffness the final deflections and response times may be reduced by an order of magnitude. A further large reduction may be caused by plastic strain rate sensitivity, as exhibited by mild steel, commercially pure titanium, and some other metals.

A way of extending of the mode technique to take account of finite deflections for nonlinear viscoplastic material, was suggested in [2] and applied to a simple model with two lumped masses. This made use of a representation of viscoplastic behavior by constitutive equations of homogeneous type [3] (without a yield condition), which are a conservative approximation and greatly simplify the analysis. The first application to a structure treated as continuous was to a clamped circular plate [4]. The present treatment extends that of [4] and includes discussion of comparison with recent test results [5].

Large deflection viscoplastic problems of dynamically loaded structures are not simple. Full details of the response are obtainable only by numerical methods; unfortunately these are still far from uniformly reliable. Neither are ad hoc short-cut methods, which can always be devised. The mode approach extended to large deflections by the use of instantaneous mode solutions, offers both practical and conceptual advantages.

2. Concepts and Equations

The mode technique in both its initial and extended forms makes use of "general integrals" which satisfy all the field equations (dynamics, kinematics, material behavior, and boundary fixing conditions) but which do not in general agree with the stipulated initial field of velocity. In particular, we may look for such a full solution in mode form, so that the velocity, for example, is written as

$$\dot{u}_i^*(x, t) = \dot{U}(t)\phi_i(x) \tag{1}$$

where $\dot{U}(t)$ is a scalar function of time and ϕ_i is a vector-valued function of the space variables x, with $i = 1,2,3$. The quantity $\dot{U}(t)$ may be defined as the velocity magnitude of particular interest, with ϕ_i normalized accordingly.

For a quite general class of material behavior expressible by equations relating stress to strain rate, a convergence principle holds [6] for <u>any</u> two full solutions of the field equations. In particular, the actual solution $\dot{u}_i(x, t)$, which satisfies specified initial conditions, approaches a solution in the mode form of Eq. (1), in the sense that the functional $\Delta(t)$ is non-increasing, where

$$\Delta(t) = \Delta[\dot{u}_i(x, t) - \dot{u}_i^*(x, t)] = \frac{1}{2}\int_V \rho(\dot{u}_i - \dot{u}_i^*)(\dot{u}_i - \dot{u}_i^*)\, dV \tag{2}$$

$$\frac{d\Delta}{dt} = -\int_V (Q_j - Q_j^*)(\dot{q}_j - \dot{q}_j^*)\, dV \leq 0 \tag{3}$$

where the integral covers the whole structure, ρ is the mass density; $Q_j, \dot{q}_j$ are generalized stress and plastic strain rate respectively in the actual solution, and Q_j^* , $\dot{q}_j^*$ the corresponding quantities in the mode solution.

The initial value $\dot{U}^o = \dot{U}(0)$ of the scalar time function in Eq. (1) is arbitrary, as far as the above properties are concerned. It can be chosen so as to minimize the initial value Δ^o ,

$$\Delta^o = \Delta(0) = \frac{1}{2}\int_V \rho(\dot{u}_i^o - \dot{U}^o\phi_i)(\dot{u}_i^o - \dot{U}^o\phi_i)\, dV \qquad (4)$$

This is a minimum when

$$\dot{U}^o = \dot{U}_m^o = \frac{\int_v \rho \dot{u}_i^o \phi_i dV}{\int_v \rho \phi_i \phi_i dV} \qquad (5)$$

Note that the functions $\phi_i(x)$ are properties of the structure, determined from the field equations and boundary conditions. When $\dot{U}^o$ is chosen according to Eq. (5) the two solutions not only approach each other but often become identical after an initial period. This means that if the final deflections are determined by integrating the mode solution Eq. (1) with initial amplitude given by (5), the error in the major final deflection is generally much less than that in initial velocity [1].

Solutions with the separated variable form of Eq. (1) can be found if the equations of dynamics and kinematics are linear and the constitutive equations are homogeneous. The latter requirement can be met by the use of homogeneous "viscous" relations [3] - which include rigid-perfectly plastic behavior as a limiting case - but the treatment of finite deflections requires nonlinear terms in the field equations which make it impossible to find a mode form solution

in the sense of Eq. (1); these equations imply that the shape functions $\phi_i(x_j)$ hold throughout the response. In contrast to these "permanent" mode solutions, "instantaneous" mode solutions may be found which satisfy the field equations with current deflections regarded as known and fixed, and for a given measure of velocity magnitude. First defined in connection with applications of the mode technique to a structure of rigid-viscoplastic material, considering small deflections [7,8], they provide a means of extending the technique to large deflections [2,4]. Although the convergence theorem Eq. (3) holds only for small deflections, the concept of starting the mode solution with amplitude given by Eq. (5) remains valid. The subsequent deflections of the solution started in this way, with initial mode shape and acceleration obtained from the small deflection equations, may be obtained approximately by fitting together a sequence of instantaneous solutions. This procedure will be outlined now for the circular plate problem.

The plate deformation is defined by displacement components $\bar{w}$, $\bar{u}$ and by generalized stresses M_r , M_θ , (bending moments) and N_r , N_θ (in-plane forces), referred to radial and circumferential coordinates $\bar{r}$, θ , Fig. 1. The plate has radius R , thickness H . We take its material behavior to be described by stress-strain rate relations appropriate for strongly rate sensitive materials with constants determined from stress-strain tests at constant strain rate. In terms of uniaxial stress σ at a fixed plastic strain level and corresponding strain rate $\dot{\epsilon}$, it is assumed that such data can be adequately represented by the equation

$$\frac{\sigma}{\sigma_o} = 1 + \left(\frac{\dot{\epsilon}}{\dot{\epsilon}_o} \right)^{1/n}, \quad \dot{\epsilon} > 0 \tag{6}$$

where σ_o , $\dot{\varepsilon}_o$, n are experimental constants which depend on the chosen plastic strain magnitude; in the case of mild steel, σ_o is conveniently taken as the lower yield stress. The experimental constants σ_o , $\dot{\varepsilon}_o$, n are used to derive the constitutive equations in terms of generalized stresses and conjugate strain rates. As will be outlined subsequently, we adopt a sandwich plate model for this derivation, assuming a generalization of Eq. (6) to describe the plane stress behavior in the two sheets, whose spacing is taken as h = H/2.

Strain rate components $\dot{\kappa}_r$, $\dot{\kappa}_\theta$ (curvature rates) and $\dot{\varepsilon}_r$, $\dot{\varepsilon}_\theta$ (middle surface extension rates) for "moderately large" deflections are taken as follows:

$$\dot{\kappa}_r = -\frac{\partial^3 \bar{w}}{\partial \bar{t} \partial \bar{r}^2} \qquad \dot{\kappa}_\theta = -\frac{1}{\bar{r}} \frac{\partial^2 \bar{w}}{\partial \bar{r} \partial \bar{t}} \tag{7a}$$

$$\dot{\varepsilon}_r = \frac{\partial^2 \bar{u}}{\partial \bar{t} \partial \bar{r}} + \frac{\partial \bar{w}}{\partial \bar{r}} \frac{\partial^2 \bar{w}}{\partial \bar{t} \partial \bar{r}} \qquad \dot{\varepsilon}_\theta = \frac{1}{\bar{r}} \frac{\partial \bar{u}}{\partial \bar{t}} \tag{7b}$$

It is convenient to define dimensionless strain rates as

$$\dot{\xi}_r = \frac{\dot{\kappa}_r}{\dot{\kappa}_o} , \quad \dot{\xi}_\theta = \frac{\dot{\kappa}_\theta}{\dot{\kappa}_o} , \quad \dot{\eta}_r = \frac{\dot{\varepsilon}_r}{\dot{\varepsilon}_o} , \quad \dot{\eta}_o = \frac{\dot{\varepsilon}_\theta}{\dot{\varepsilon}_o} \tag{8}$$

where $\dot{\kappa}_o = \frac{2\dot{\varepsilon}_o}{h} = \frac{4\dot{\varepsilon}_o}{H}$. In terms of dimensionless displacements and other variables, these are

$$\dot{\xi}_r = -\frac{1}{\alpha} \dot{w}'' , \qquad \dot{\xi}_\theta = -\frac{1}{\alpha} \frac{1}{r} \dot{w}' \tag{9a}$$

$$\dot{\eta}_r = \frac{2}{\alpha} \left(\frac{2R}{H} \dot{u}' + w' \dot{w}' \right) , \quad \dot{\eta}_\theta = \frac{4}{\alpha} \frac{R}{H} \frac{\dot{u}}{r} \tag{9b}$$

where

$$w = \frac{2\bar{w}}{H} \qquad u = \frac{2\bar{u}}{H} \qquad r = \frac{\bar{r}}{R}, \qquad t = \frac{\bar{t}}{\tau}$$

$$\tau = R\sqrt{\frac{2\rho}{\sigma_o}}, \qquad \alpha = \frac{8\dot{\epsilon}_o R^2 \tau}{H^2} = \frac{8\dot{\epsilon}_o R^3}{H^2}\sqrt{\frac{2\rho}{\sigma_o}} \tag{10a,b}$$

where $\dot{f} \equiv \partial f/\partial t$, $f' \equiv \partial f/\partial r$, and ρ is the mass per unit volume. With this definition of reference time τ, the equation of energy dissipation rate is

$$-\int_o^1 (\ddot{w}w + \ddot{u}u)rdr = \alpha \int (m_r\dot{\xi}_r + n_r\dot{\eta}_r + m_\theta\dot{\xi}_\theta + n_\theta\dot{\eta}_\theta)\, rdr \tag{11}$$

where we have defined dimensionless stresses as

$$m_r = \frac{M_r}{M_o}, \quad m_\theta = \frac{M_\theta}{M_o}, \quad n_r = \frac{N_r}{N_o}, \quad n_\theta = \frac{N_\theta}{N_o} \tag{12}$$

with $M_o = \sigma_o H^2/4$, $N_o = \sigma_o H$; these are fully plastic bending moment and axial force per unit length, respectively, corresponding to the stress σ_o defined in Eq. (6).

Consistent with Eqs. (11) and (9), the equations of dynamics are

$$(rm_r)'' - m_\theta' + 2(rn_r w')' = r\ddot{w} \tag{13a}$$

$$(rn_r)' - n_\theta = \frac{H}{4R} r\ddot{u} \tag{13b}$$

with boundary conditions

$$\dot{w}(1,t) = \dot{w}'(1,t) = 0 \tag{14a}$$

$$\dot{u}(0,t) = \dot{u}(1,t) = 0 \tag{14b}$$

$$m_r(0,t) = m_\theta(0,t) \tag{14c}$$

Finally we write suitable constitutive equations. We want these to represent the main features of rate sensitive plastic behavior and to reduce to rigid-perfectly plastic behavior as a limiting case. Strain rate test data of the metals of present interest can be quite accurately represented by Eq. (6). As already mentioned, a sandwich model is used to derive the stress-strain rate relations for our plate, based on this behavior which is readily generalized (following Perzyna [9]), adopting a Mises yield condition for plane stress. Use of a sandwich model, with constants so that both simple bending and simple extension of the uniform plate are correctly described, is an artifice which simplifies the equations and is conservative. A further simplifying and conservative artifice is the use of homogeneous stress-strain rate relations. Thus the generalized form of Eq. (6) for plane stress is

$$\frac{\sigma_\alpha}{\sigma_o'} = \left[\frac{g(\dot{\varepsilon}_\beta)}{\dot{\varepsilon}_o}\right]^{1/n'} \frac{\partial g}{\partial \dot{\varepsilon}_\alpha} \tag{15a}$$

where

$$g(\dot{\varepsilon}_\beta) = \frac{2}{\sqrt{3}} (\dot{\varepsilon}_r^2 + \dot{\varepsilon}_r\dot{\varepsilon}_\theta + \dot{\varepsilon}_\theta^2)^{1/2} \tag{15b}$$

and α, β take values r or θ. The new constants σ_o', n' are found from the experimental constants σ_o, $\dot{\varepsilon}_o$, n so that the homogeneous replacement of Eq. (6) has common stress and derivative $d\sigma/d\dot{\varepsilon}$ at a chosen strain rate. These

matching conditions make the homogeneous forms an accurate and conservative replacement [2,3]; they are obtained by taking $n' = \nu n$, $\sigma_o \quad \mu\sigma_o$, where

$$\nu = \frac{n'}{n} = \frac{1 + \tilde{v}_o^{1/n}}{\tilde{v}_o^{1/n}} \quad ; \qquad \mu = \frac{\sigma_o'}{\sigma_o} = \frac{1 + \tilde{v}_o^{1/n}}{\tilde{v}_o^{1/\nu n}} \tag{16a,b}$$

where

$$\tilde{v}_o = g(\tilde{\dot{\varepsilon}}_\alpha)$$

and $\tilde{\dot{\varepsilon}}_\alpha$ denotes the strain rate state at which the matching is made. (Errors due to these and other idealizations and approximations are discussed in a later section). From Eqs. (15) and (16) the sandwich beam model leads to equations which allow the generalized stresses Q_j to be derived from a potential function of strain rates $\dot{q}_j$; we write

$$Q_j = \frac{\partial \omega}{\partial \dot{q}_j} \quad ; \quad \omega(\dot{q}_j) = \frac{n'}{2(1+n')} \left[\chi_+^{1+1/n'} + \chi_-^{1+1/n'} \right] \tag{17}$$

where $Q_j = (m_r \ , \ n_r \ , \ m_\theta \ , \ n_\theta)$; $\dot{q}_j = (\dot{\xi}_r \ , \ \dot{\eta}_r \ , \ \dot{\xi}_\theta \ , \ \dot{\eta}_\theta)$

and

$$\chi_\pm = \frac{2}{\sqrt{3}} \ \mu \left[(\dot{\eta}_r \pm \dot{\xi}_r)^2 + (\dot{\eta}_r \pm \xi_r)(\dot{\eta}_\theta \pm \xi_\theta) + (\dot{\eta}_\theta \pm \xi_\theta)^2 \right]^{1/2} \tag{18}$$

Conversely, the strain rates $\dot{q}_j$ may be derived from a potential function of the stresses $\Psi(Q_j)$. Further details are given in [4] including illustrations of surfaces $\Psi(Q_j) =$ constant for our problem.

We now look for a solution in mode form, and write the velocity components as

$$\dot{w}(r,t) = \dot{w}_*(t)\phi_1(r) \tag{19a}$$

$$\dot{u}(r,t) = \dot{w}_*(t)\phi_2(r) \tag{19b}$$

We take $\phi_1(0) = 1$, so that $\dot{w}_*(t)$ denotes the velocity (nondimensional) of the midpoint of the plate. Because the strain rate-velocity expressions are linear in the velocities and the stress-strain rate relations are homogeneous, we can write the latter in compact form as

$$Q_i = \mu\left(\frac{\dot{w}_*}{\alpha}\right)^{1/n'} B_{ij}k_j \tag{20a}$$

where $i, j = 1,2,3,4$, and summation over a repeated suffix is implied,

$$Q_i = \left(m_r \quad n_r \quad m_\theta \quad n_\theta \right)$$

$$k_j = \left(-\phi_1'' \quad \frac{4R}{H}\phi_2' + 2w'\phi_1' \quad -\frac{1}{r}\phi_1' \quad \frac{4R}{H}\frac{1}{r}\phi_2 \right) \tag{21b}$$

$$B_{ij} = \begin{bmatrix} \frac{2}{3}(\tilde{\chi}_+ + \tilde{\chi}_-) & \frac{2}{3}(\tilde{\chi}_+ - \tilde{\chi}_-) & \frac{1}{3}(\tilde{\chi}_+ + \tilde{\chi}_-) & \frac{1}{3}(\tilde{\chi}_+ + \tilde{\chi}_-) \\ \frac{2}{3}(\tilde{\chi}_+ - \tilde{\chi}_-) & \frac{2}{3}(\tilde{\chi}_+ + \tilde{\chi}_-) & \frac{1}{3}(\tilde{\chi}_+ - \tilde{\chi}_-) & \frac{1}{3}(\tilde{\chi}_+ + \tilde{\chi}_-) \\ \frac{1}{3}(\tilde{\chi}_+ + \tilde{\chi}_-) & \frac{1}{3}(\tilde{\chi}_+ - \tilde{\chi}_-) & \frac{2}{3}(\tilde{\chi}_+ + \tilde{\chi}_-) & \frac{2}{3}(\tilde{\chi}_+ - \tilde{\chi}_-) \\ \frac{1}{3}(\tilde{\chi}_+ - \tilde{\chi}_-) & \frac{1}{3}(\tilde{\chi}_+ + \tilde{\chi}_-) & \frac{2}{3}(\tilde{\chi}_+ - \tilde{\chi}_-) & \frac{2}{3}(\tilde{\chi}_+ + \tilde{\chi}_-) \end{bmatrix}$$

$$\tilde{\chi}_{\pm} = \left\{ \frac{2}{\sqrt{3}} \left[(k_1 \pm k_2)^2 + (k_1 \pm k_2)(k_3 \pm k_4) + (k_3 \pm k_4)^2 \right] \right\}^{\frac{1}{n'}-1} \tag{21d}$$

In terms of these quantities the energy rate equation is

$$-w_* = \mu \left(\frac{\ddot{w}_*}{\alpha} \right)^{\frac{1}{n'}} \left\{ \frac{\int_0^1 B_{ij} k_i k_j r dr}{\int_0^1 (\phi_1^2 + \phi_2^2) r dr} \right\} \tag{22}$$

The dynamical equations (13) take the forms

$$\mu \left(\frac{\dot{w}_*}{\alpha} \right)^{\frac{1}{n'}} \left[(rB_{2j}k_j)'' - (B_{3j}k_j)' + 2(rB_{2j}k_j w')' \right] = r\ddot{w}_* \phi_1 \tag{23a}$$

$$\mu \left(\frac{\dot{w}_*}{\alpha} \right)^{\frac{1}{n'}} \left[(rB_{2j}k_j)' - B_{4j}k_j \right] = \frac{H}{4R} r\ddot{w}_* \phi_2 \tag{23b}$$

Inspection of Eqs. (23) shows that if $w'(r,t)$ is either zero or treated as known and independent of time, the equations are separable into three ordinary differential equations

$$w_* = - A\mu \left(\frac{\dot{w}_*}{\alpha} \right)^{1/n'} \tag{24a}$$

$$L_1[\phi_1, \phi_2, w'] + Ar\phi_1 = 0 \tag{24b}$$

$$L_2[\phi_1, \phi_2, w'] + \frac{H}{4R} Ar\phi_2 = 0 \tag{24c}$$

where L_1, L_2 are the expressions in brackets on the left hand sides of Eq. (23a) and (23b), respectively, and A is a constant. Evidently if $w'(r,t)$ is

taken as fixed we have a nonlinear eigen-problem in which the constant A is the eigenvalue, and the shape functions $\phi_1(r)$, $\phi_2(r)$ are eigenfunctions. Note that A is given by the quotient in brackets in Eq. (22) in terms of ϕ_1 , ϕ_2 , and w'.

How to obtain a mode form solution from a sequence of instantaneous modes can now be seen. The solution starts with a choice of initial value $\dot{w}_*^o = \dot{w}_*(0)$. At $t = 0$ the deflection field and slope $w'(r,0)$ are zero. The initial mode from solution has $\phi_2(r) = 0$, and $\phi_1(r)$ can be found without difficulty [4,10], together with the corresponding value of A . The secular equation Eq. (24a) can readily be integrated if A is held constant, to provide a rough "small deflection" solution.

A much better solution for finite deflections is obtained as follows. Suppose at time t the eigen-problem has been solved, giving $\dot{w}_*(t)$, $\ddot{w}_*(t)$, $\overset{<t>}{\phi_1}(r)$, $\overset{<t>}{\phi_1'}(r)$, the deflection $w(r,t)$, and slope $w'(r,t)$. Approximate deflection and slope fields at $t + \Delta t$ are

$$w(r_1 t+\Delta t) \tilde{=} w(r,t) + (\Delta t)\dot{w}_*(t)\overset{<t>}{\phi_1}(r) + \tfrac{1}{2}(\Delta t)^2\ddot{w}_*(t)\overset{<t>}{\phi_1}(r) \qquad (25a)$$

$$w'(r,t+\Delta t) \tilde{=} w'(r,t) + (\Delta t)\dot{w}_*(t)\overset{<t>}{\phi_1'}(r) + \tfrac{1}{2}(\Delta t)^2\ddot{w}_*(t)\overset{<t>}{\phi_1'}(r) \qquad (25b)$$

With the approximate field $w'(r,t+\Delta t)$ given by Eq. (25b), the eigen-problem for $t + \Delta t$ can be solved, furnishing approximate values of $\dot{w}_*(t+\Delta t)$, $\ddot{w}_*(t+\Delta t)$, $\overset{<t+\Delta t>}{\phi_1}(r)$, $\overset{<t+\Delta t>}{\phi_1'}(r)$, etc. With these, better approximations can be written as

$$w(r,t+\Delta t) = w(r,t) + \frac{1}{2}(\Delta t)\left[\dot{w}_*^{<t>}(t)\phi_1(r) + \dot{w}_*^{<t+\Delta t>}(t+\Delta t)\phi_1(r)\right] \tag{26a}$$

$$w'(r,t+\Delta t) = w'(r,t) + \frac{1}{2}(\Delta t)\left[\dot{w}_*^{<t>}(t)\phi_1'(r) + \dot{w}_*^{<t+\Delta t>}(t+\Delta t)\phi_1'(r)\right] \tag{26b}$$

This process can be repeated until steady values are reached. It is started at $t = 0$ when $w(r,0) = w'(r,0) = 0$.

An eigen-problem must be solved for each field w' in this process. In [4] this was done by an iterative scheme, in which the terms of higher order derivatives in Eqs. (13) were written as functions of the lower order terms, and integrated numerically over the radial coordinate. This gave an essentially exact solution at small computer cost when there was no difficulty with convergence, as was the case at small magnitudes of $\dot{w}_*^o$. At larger values of $\dot{w}_*^o$, such that the central deflection exceeded about 4 thicknesses, the acceleration magnitude exhibited poor convergence, although the deflections showed little change with increased numbers of iteration cycles. An alternative procedure using finite elements was therefore devised, taking cubic and linear expressions for ϕ_1 and ϕ_2, respectively, in each element. Iterations were required to obtain the unknown slope w' in various matrices. Some difficulties with convergence still occurred at the largest deflections.

We have emphasized here the determination of mode responses, i.e., the integration of the field equations of the structure whose starting velocities have the form of the initial mode shape (appropriate to zero deflections and to the

chosen initial velocity amplitude), and which reach large deflection magnitudes in the course of the response. We have outlined an approximate integration technique using a sequence of instantaneous modes (each appropriate to the current deflections and velocity amplitude). This technique appears promising as an efficient and flexible scheme to obtain the final deflections and the duration of the motion, among other quantities. Other methods may be used, of course, including numerical codes if available.

To obtain the mode solution which provides the best approximation for a particular problem, for which an initial transverse velocity field $V(r)$ is prescribed, the amplitude $\dot{w}^o_*$ of the initial mode velocity field must be found by the minimizing technique expressed by Eq. (5): using nondimensional variables,

$$\dot{w}^o_* = \int_o^1 \dot{w}^o(r)\phi_1 r dr \Big/ \int_o^1 \phi_1^2 r dr \qquad (27)$$

where $\dot{w}^o(r) = V(r)(2\tau/H)$, using the reference time τ defined in Eq. (10a), is the prescribed initial velocity field in nondimensional form. The integration in dimensionless variables can be carried out if the parameters α, n, and R/H are specified, where α is defined in Eq. (10b) and n implicitly in Eq. (6). It is seen that α depends on the size R as well as the shape R/H of the structure and on the material constants $\dot{\varepsilon}_o$, σ_o, ρ.

In principle, such an integration to obtain the mode response should be repeated for each case of interest, i.e., for each $V(r)$, R, R/H, σ_o $\dot{\varepsilon}_o$, etc. When an assessment of deformation for severe pulse loads is required, there are often many uncertainties about the loading intensity and distribution over the structure, and about the structure itself, particularly concerning its material behavior at high strain rates. Hence one wants not an isolated calculation but curves showing how the deformations depend on various parameters as they vary

over appropriate ranges. The mode approximation technique is particularly suited to looking at variations over such ranges with a minimum of calculations.

A set of mode responses in nondimensional form, giving for example a curve of final deflection ratio w_*^f/H as a function of initial mode velocity amplitude $\dot{w}_*^o$, for "representative" values of α, n, and R/H, provides a sort of "master response function" from which a considerable range of particular cases can be examined with trivial further calculations. This is due partly to the basic device of the mode approximation concept of matching mode amplitude to an arbitrary initial velocity field as in Eqs. (5, 27), and partly to the insensitivity of the nondimensional mode solution to various parameters. In particular, the solution depends very weakly on α, since α appears in the equations only as $\alpha^{1/n'}$ (where n' is usually in the neighborhood of 10). Finally, the initial mode shape function $\phi_1(r) = \overset{<o>}{\phi}(r)$ is insensitive to the initial amplitude $\dot{w}_*^o$ as well as to α. These points, which are important for practical use, are illustrated below.

3. Application to Tests

In tests [5] on fully clamped plates of mild steel and titanium, explosive loading was applied by detonating a disk of explosive sheet (Detasheet) fixed centrally on the plate and separated from it by a buffer pad of styrofoam, Fig. 2. The total impulse applied to the plate was measured in each test by a ballistic pendulum. It was assumed that velocities $V(r)$ were imposed, such that

$$\begin{aligned} V(r) &= V_o \quad \text{for} \quad 0 \leq r \leq a \\ V(r) &= 0 \quad \text{for} \quad a \leq r \leq R \end{aligned} \tag{28}$$

where a is the radius of the disk of explosive. Further it was taken that

$$V_o = \frac{I}{\pi a^2 H \rho} \tag{29}$$

where I is the measured impulse, and ρ is the mass density of the plate of thickness H. This assumes that reaction stresses in the plate are negligible during the pulse, and that the explosive pressures are uniform inside radius a and zero outside. It is further assumed that the pressure pulse is so short that it can be treated as a pure impulse. The expression for initial mode velocity amplitude then gives the relation

$$\frac{\dot{w}_*^o}{\dot{w}_o} = \int_o^{a/R} \phi_1 r dr \Big/ \int_o^1 \phi_1^2 r dr \equiv J\left(\frac{a}{R}\right) \tag{30}$$

where $\dot{w}_o = \frac{2\tau}{H} V_o$. From this definition, combined with Eqs. (10a) and (29), we obtain the relation

$$\dot{w}_o = \frac{2R}{H}\sqrt{\frac{2\rho}{\sigma_o}}\, V_o = \frac{2\sqrt{2}}{\pi}\,\frac{RI}{H^2 a^2 \sqrt{\rho\sigma_o}} \tag{31}$$

Suppose now the final midpoint deflections w_*^f/H of the mode response have been computed as a function of initial mode amplitude $\dot{w}_*^o$, for suitable values of α, n, and R/H. Figure 3 shows two such "master" solutions for steel and titanium plates, using numerical values in Table 1. Fig. 4 shows nondimensional curves of mode velocity amplitude as function of time. From the curves of Fig. 3, Eqs. (30) and (31) enable us to obtain curves of deflection as function of applied impulse I for any assumed impulsive pressure distribution, and to assess the importance of uncertainties in the material and geometrical descriptions. The procedure is inverse; rather than specifying the impulse and determining the corresponding deflection, the latter is chosen first. The ratio w_*^f/H determines $\dot{w}_*^o$ from the appropriate curve of Fig. 3. The value of $\dot{w}_o$ is then obtained from Eq. (30) for the specified ratio a/R of the impulsive loading. In principle, the ratio $\dot{w}_*^o/\dot{w}_o$ depends on $\dot{w}_*^o$, since the initial shape function

Table 1

		Steel	Titanium
Strain Rate Constant[1]	σ_o psi	32,400[2]	36,400 at ϵ^p = 1% (35,200 long., 37,700 trans.) 38,500 at ϵ^p = 2% (37,800 long., 39,200 trans.)
Strain Rate Constant[1]	$\dot{\epsilon}_o$ sec^{-1}	40	120
Strain Rate Constant[1]	n	5	9
Mass Density	ρ lb sec^{2}in.$^{-4}$	0.73×10^{-3}	0.42×10^{-3}
Plate Radius	R in.	1.25	1.25
Plate Thickness (Average)	H in.	0.076	0.092
$\frac{8R^3}{H^2}\dot{\epsilon}_o\sqrt{\frac{2\rho}{\sigma_o}}$	α	23.0	33.8

[1] As used in Eq. (3).

[2] Lower yield stress.

$\phi_1(r)$ for the viscoplastic material depends on the initial velocity as well as material parameters. In fact, the dependence of ϕ_1 on $\dot{w}_*^o$ is found to be exceedingly weak, and a single curve for each plate can be drawn showing $\dot{w}_*^o/\dot{w}_o$ as a function of a/R. These are plotted in Fig. 5. The two curves are indistinguishable over most of the range, showing that the initial shape function $\phi_1(r)$ is insensitive to all the parameters. Writing $\dot{w}_*/\dot{w}_o$ as J(a/R) from Eq. (30), we find I from Eq. (31) as

$$I = \left\{\frac{\pi}{2\sqrt{2}} H^2 R\sqrt{\rho\sigma_o}\right\} \frac{a^2/R^2}{J(a/R)} \dot{w}_*^o \qquad (32)$$

Obviously the same procedure for obtaining the deflection as function of impulse (both in physical units) can be carried out for any assumed initial velocity form V(r).

Suppose now we wish to examine possible variations in some of the physical parameters assumed in the above calculation. There are many quantities whose values are uncertain. For example, in the calculation we have assumed the initial impulsive pressures to give rise to uniform velocity V_o inside a circle of radius a and zero velocity outside this radius, with a taken as the radius of the disk of explosive sheet. Series of tests were conducted with nominal a/R = 1/3, 1/2, and 1. The test arrangement as sketched in Fig. 2 makes it evident that the actual loading area must differ from the nominal one; there must be a "shadow effect" due to the buffer pad. (In practical problems of explosive loading on structures, as opposed to laboratory experiments, far more uncertainty than this would be expected). Other somewhat uncertain quantities are the parameters of strain rate sensitivity σ_o , n , $\dot{\varepsilon}_o$, obtained from stress-strain tests over a range of strain rates. These pertain to a fixed plastic strain magnitude, which should be chosen so as to conform

reasonably well with the actual maximum strains. (For mild steel we have used the lower yield stress, rather than stress at fixed plastic strain). As "nominal" value for the titanium plates we took σ_o = 36,000 psi corresponding to 1 percent strain.

The sensitivity of an estimated impulse-deflection curve to moderate changes in the parameters a/R and σ_o can now be examined simply by changing either of these quantities in evaluating I from Eq. (32). Thus the effect of changing a/R by 20 percent (from 0.33 to 0.40) is obtained by reading a new point for $J(0.40)$ from the curve in Fig. 5. Since both a^2/R^2 and $J(a/R)$ increase, and I depends on their ratio, the effect is small. This is illustrated in Fig. 6 together with test results, to be discussed later. Sensitivity to a change in the magnitude σ_o is of less interest for steel than for titanium whose strain hardening slope is larger [5]. If the fixed plastic strain level is taken as 2 percent rather than 1 percent, the appropriate average value of σ_o is about 39,000 psi. Equation (32) shows that I is proprotional to $\sqrt{\sigma_o}$; the small change is shown by the shift in the curve in Fig. 7 when 36,000 is replaced by 39,000. Note that the parameter α is changed by a like amount, but the effect on the "master response curve" of a 4 percent change in α is effectively zero, because of the weak dependence already mentioned.

4. Comparison with Experiments

The experiments reported in [5] were planned so that the concepts and assumptions of the extended mode approximation technique could be checked directly. The intrinsic error in the estimation of deflections of the fully clamped plate is represented by Eq. (30) for initial velocity distributed as in Eq. (29); equivalent expressions for $\dot{w}_*^o/\dot{w}_o$ for other types of velocity pattern are readily

derived. The plot of $\dot{w}^{o}_{*}/\dot{w}_{o}$ in Fig. 5 shows that this ratio is positive or negative as a/R is larger or smaller than about 0.47. For impulsive pressures over the whole plate (a/R = 1) the error is positive (conservative), while for a/R = 1/3 the error is negative since $\dot{w}^{o}_{*}/\dot{w}_{o}$ is about 0.6. For a/R = 1/2, the intrinsic error should be nearly zero.

The tests used nominal values of a/R equal to 1/3, 1/2 and 1, using steel and titanium plates, and impulse magnitudes such that final deflections up to more than six thicknesses were produced. Examples of these test series are shown in Figs. 6-11, where Fig. 9 shows a typical final deflected shape and Figs.10,11 show examples of response times as function of impulse, in two series of tests. More results and details of the materials and techniques are given in [5].

The plots of final central deflection as function of impulse in Figs. 6-8 illustrate the results for the three nominal a/R values. If no other important idealization or error were involved, the full curves showing deflection estimates from the finite-deflection mode theory would show the intrinsic error; for a/R = 1/3 and 1 the estimated deflections would lie below and above the test values, while for a/R = 1/2 the estimates would be close to the observed values. No such trends are observed. Fig. 7 (for a/R = 1/2) shows test deflections substantially smaller than the mode theory prediction. For a/R = 1, the observed deflections lie above the predicted curve, while for a/R = 1/3 they lie below, the reverse of the intrinsic error. (In these curves the curves labelled "small deflection" are from simple bending theory, and exhibit much larger errors).

These anomalous results point to the importance of other error sources. There are two kinds. "Experimental" errors are ones in which one or more assumed conditions of the tests are not met. "Theoretical" errors also are present,

apart from the intrinsic error already discussed, because of various idealizations and approximations in carrying out the mode solution to obtain finite deflections.

Of the possible experimental errors only one is believed significant. The condition of full edge fixity was not satisfied in the tests where impulsive pressures were applied over the entire plate ($a/R = 1$). The heavy clamping frame sketched in Fig. 2 used eight 1/4 in. bolts. The friction forces on the clamped portion of the plate were adequate to prevent slipping at the smaller loads used for $a/R = 1/3$ and $1/2$, but in the tests with $a/R = 1$ inward displacements at the specimen edge as much as 1/16 in. were measured. These led to greatly increased deflections, as indicated by the curves for "small deflections" in Figs. 6-8, from a theory assuming absence of membrane stresses. The negative error of the estimated deflections by the mode technique shown in Fig. 8 are due to swamping of all other errors by this failure in the assumed constraint. We mention that the test series on titanium plates [5] also showed anomalously high values of deflections in tests at $a/R = 1$, but the test points fell slightly below rather than well above the mode response curves.

Turning to errors in the theory, we summarize below those expected due to idealizations and approximations made in implementing the mode technique. Unlike the intrinsic error already discussed, these are almost all positive (conservative) although in some cases the argument is conjectural. This seems unavoidable in discussing an estimation technique at this stage.

(a) Material Behavior

(1) Elastic strains are omitted as negligible compared with plastic strains. For such a rigid-viscoplastic theory to be realistic, an energy ratio criterion has been postulated. Here the ratio of initial kinetic energy to the maximum elastic strain energy is

greater than 10 for impulses greater than about 0.2 lb-sec, in all cases. Since the criterion appears to be well satisfied for all of the tests reported in [5], the error due to neglect of elastic deformations should be less than 10 percent even for the smallest impulses. This may be argued to be a positive error when the load pulse is short, as here [11].

(2) Constitutive equations are derived from a sandwich model with separation between sheets half the uniform plate thickness H. With this choice, the stress-strain rate relations are correct for pure tension/compression and for pure bending, and conservative for general stress states in the sense that smaller stress levels are required for a fixed dissipation rate.

(3) A homogeneous viscous stress-strain rate representation is used, without a yield condition, and matched to the viscoplastic form in such a way that stress magnitudes are very close to the "correct" ones near an assigned strain rate, and always below them. The error is positive on this account [2,3].

(4) The constitutive equations relate stress and strain rate states explicitly, influences of strain hardening being implicit only. With the choices we have made of fixed strain level (or of lower yield stress in the case of steel) the error is positive. Its magnitude can be estimated, as has been shown.

(5) Strain rate history effects are neglected; the stress is written as a function of instantaneous strain rate, and the constitutive equations are derived from tests at approximately constant strain rate. Strain rate jump tests [12,13] among others demonstrate

that the stress is not a function only of current strain and strain rate, and some error must therefore arise. The information from tests is meagre and the behavior is complex, so that no firm statements can be made about the magnitude or sign of the error. The present structural problems involve high strain rates which are rapidly imposed by the dynamic loading and then decrease to zero. It may be conjectured that the neglect of prior straining history leads to a positive error in the deflection estimate, the stress levels being underestimated. (This follows from interpretations of test data either by choosing plastic work as a state variable [14] or regarding dynamic recovery as the essential process [15].)

(b) Numerical or Theoretical Approximations

(6) The mode technique, as applied here to finite deflections, involves a sequence of modal fields of velocity and acceleration which do not fit together continuously except at the plate center, where the mode velocity is $\dot{w}_*(t)$. These mode form solutions correspond to a minimum dissipation rate for a fixed kinetic energy [7,8,12], hence to slower deceleration magnitudes than the actual solution. On this ground, the error resulting from the instantaneous mode technique is expected to be positive.

(7) The numerical determination of mode shapes and accelerations required iterations. At each stage first approximations were used for the new deflection field and for the effective strain rate (furnishing μ and ν); solution of the resulting eigen-problem then led to improved values which were used to start a second

cycle, etc. Convergence was very slow at the largest deflections. Ten iteration cycles were mainly used, except for a few trial calculations. These were not enough at the largest deflection magnitudes, and the deflections so calculated are too large (decreasing magnitudes being obtained by additional cycles). The finite element form of the equations involves further errors of unknown sign and magnitude. Thus the net error due to numerical causes (at the largest deflections) is probably positive, but this is uncertain.

(8) The field equations include finite deflection terms which are consistent but approximate, as in the von Karman plate equations. They are strictly valid for moderately large deflections, but are expected to be very reliable for all the deflection magnitudes concerned here, where the maximum deflection is less than 1/5 the diameter.

(9) Finally, the explosive pressure pulse is treated as impulsive, i.e., delivering finite impulse with zero duration. This idealization in which a single pulse of arbitrary shape is replaced by a pure impulse, is known to lead to over-estimates of final deflections of structures treated as rigid-perfectly plastic by small deflection theory [17]. A simple model of this type gives the error as roughly equal to the ratio of the pulse duration to the duration of motion of the structure. Intuitively, similar results should hold true for the closely related rigid-viscous or viscoplastic behavior treated here, and for large deflection problems. The tests of [5] involve pulses whose duration was estimated at less than 10 μsec., so the positive error from the pure impulse idealization might be around 10 percent.

It is remarkable that the possible errors introduced by the idealization and approximations listed above are almost all positive. The exceptions are items (7) and (8); there is no reason to suppose that these are predominant. Again, no apology is made for the fact that the arguments about some of the errors are conjectural. This seems unavoidable when one is trying to assess an approximation technique by comparison with actual measured behavior of structures. One can hardly make rigorous statements unless one is dealing with "exact" theory, or making comparisons with quantities furnished by a computer program. Even then, rigorous statements may be illusory, given the fictional nature of computer outputs.

Comparisons with measured response times are typified by the results shown in Figs. 10 and 11. In the tests [5] a "condenser microphone" device was used to obtain information about time history of deflection. This consisted of a brass plate held on an insulated rod, with geometry as indicated in Fig. 2. Deflection of the plate caused roughly proportional capacitance changes, which were recorded. Quantitative accuracy was not possible, but two times of interest were obtained, namely the time to reach maximum deflection t_f' , and the time t_f'' when the (estimated) permanent deflection magnitude was reached on the initial rise of the signal. These two times are plotted in Figs. 10 and 11 as function of test impulse, together with the time t_f at which motion ceases according to the mode approximation technique. According to this technique the response time first increases with impulse, reaches a maximum, and then slowly decreases. This behavior is readily understandable: at large deflections where membrane effects dominate, the plate is much stiffer than in the simple bending range. The response time then depends mainly on the maximum tensile forces rather than on the impulse. Since the material is strain rate dependent, the membrane forces increase with impulse and the response duration decreases. The

particular test series shown for illustration in Fig. 11 shows this decrease plainly. However, this is exceptional in that most of the similar plots in [5] are similar to those in Fig. 10 which shows virtual independence of the measured times with impulse. In all cases the agreement of test times with the maximum response times given by the extended mode technique is quite good, while the response times predicted by the small deflection theory have no resemblance to the observed times.

5. Conclusions

We have reviewed the application of the mode approximation technique to estimate finite viscoplastic deflections of an impulsively loaded fully clamped circular plate. The concept of a "master solution" for a range of initial mode velocity amplitudes, taking representative values of the dimensionless parameters, is shown to reduce the calculations to a minimum, and enhances the efficiency of the method. Comparisons with tests on plates of steel and titanium are made, and discussed with particular reference to possible errors in the estimation technique. Certain errors are intrinsic in the method; others occur as result of idealizations and approximations in implementing it. The tests substantiate the expectation that the errors of the latter type are predominately positive, i.e., tending to over-estimate the final deflections. The intrinsic errors are either positive or negative, depending on the distribution of impulsive pressure; they could not be identified in the test results, apparently being outweighed by the other type. The tests show that the technique as applied is conservative when the assumed edge constraint condition was satisfied, and close enough to the observed deflections to permit confidence in practical applications.

References

1. Martin, J. B. and Symonds, P. S., "Mode Approximations for Impulsively Loaded Rigid-Plastic Structures," J. Eng. Mech. Div. Proc. ASCE, Vol. 92, No. EM5, pp. 43-66.

2. Symonds, P. S. and Chon, C. T., "Approximation Techniques for Impulsive Loading of Structures of Time-Dependent Plastic Behavior With Finite Deflections," Proc. Oxford Conf. "Mechanical Properties of Materials at High Strain Rates," Inst. of Physics Conf. Ser. No. 21, Dec. 1974, pp. 299-315, edited by J. Harding.

3. Symonds, P. S., "Approximation Techniques for Impulsively Loaded Structures of Rate Sensitive Plastic Behavior," SIAM J. Appl. Math, Vol. 25, No. 3, Nov. 1973, pp. 462-273.

4. Chon, C. T. and Symonds, P. S., "Large Dynamic Deflection of Plates by Mode Method," J. of the Eng. Mech. Div., Proc. ASCE., Vol. 103, No. #M1, pp. 3-14, Feb. 1977.

5. Bodner, S. R. and Symonds, P. S., "Experiments on Viscoplastic Response of Circular Plates to Impulsive Loading," Tech. Report N00014-0860/6 for Brown University under Grant NSF 74-21258 and Contract N00014-75-C-0860, pp. 1-16.

6. Martin, J. B., "A Note on Uniqueness of Solutions for Dynamically Loaded Rigid-Plastic and Rigid-Viscoplastic Continua", J. Appl. Mech., Vol. 33, pp. 207-209, 1966.

7. Lee, L. S. S. and Martin, J. B., "Approximate Solutions of Impulsively Loaded Structures of a Rate Sensitive Material," J. Appl. Math. Physics (ZAMP) Vol. 21, pp. 1011-1032, 1970.

8. Lee, L. S. S., "Mode Responses of Dynamically Loaded Structures," J. Appl. Mech., Vol. 39, pp. 904-910, 1972.

9. Perzyna, P., "The Constitutive Equations for Rate Sensitive Plastic Materials," Q. Appl. Math., Vol. 20, pp. 321-331, 1963.

10. Symonds, P. S. and Chon, C. T., "On Dynamic Plastic Mode Form Solutions," Tech. Report for Brown University under Grant No. NSF 74-21258 and Contract N00014-75-C-0860/2, pp. 1-18.

11. Symonds, P. S., "Survey of Methods of Analysis for Plastic Deformation of Structures Under Dynamic Loading," Report BU/NSRDC/1-67, from Brown University to Office of Naval Research, Naval Ship Research and Development Center, Contract Nonr 3248(01)(X), June 1967.

12. Symonds, P. S. and Wierzbicki, T., "On an Extremum Principle for Mode Form Solutions in Plastic Structural Dynamics," J. Appl. Mech. Vol. 42, No. 3, Sept. 1975, pp. 630-640.

13. Frantz, R. A., Jr., and Duffy, J., "The Dynamic Stress-Strain Behavior of Torsion of 1100-0 Aluminum Subjected to a Sharp Increase in Strain Rate," J. Appl. Mech., Vol. 39, No. 4, 1972, pp. 939-945.

14. Campbell, J. D. and Eleiche, A. M., "The Influence of Strain-Rate History and Temperature on the Shear Strength of Copper, Titanium and Mild Steel," Dept. of Eng. Science, U. of Oxford, Tech. Report AFML-TR-76-90, Final Report for Period 1 Feb. - 31 July 1975, pp. 1-101.

15. Bodner, S. R. and Partom, Y., "Dynamic Inelastic Properties of Materials: Part II - Representation of Time Dependent Characteristics of Metals," ICAS Paper No. 72-28, Eighth Congress of the International Council of the Aeronautical Sciences, Internationaal Congrescentrum Rai-Amsterdam, The Netherlands, Aug. 28 to Sept. 2, 1972, pp. 9-14.

16. Klepaczko, J. and Duffy, J., "Strain Rate and Temperature Memory Effects for Some Polycrystalline fcc Metals," Conf. Series No. 21, The Institute of Physics, Mechanical Properties at High Rates of Strain, 1974, pp. 91-101.

17. Youngdahl, C. K., "Correlation Parameters for Eliminating the Effect of Pulse Shape on Dynamic Plastic Deformation," J. Appl. Mech., Vol. 37, pp. 744-752, 1970.

Captions for Figures

Figure

1 Notation for axially symmetric deformations - physical units.

2 Clamped plate as used in experiments [5].

3 "Master response curves" for steel and titanium plates. $\bar{w}_*^f/H$ is nondimensional final displacement at center, $\dot{\bar{w}}_*^o = V_*^o\tau/H$ is nondimensional initial mode velocity amplitude.

4 Illustrative curves of mode velocity amplitude versus time.

5 Ratio of initial mode velocity amplitude $\dot{\bar{w}}_*^o$ to specified initial velocity magnitude $\dot{w}_o$ (nondimensional), given by mode technique.

6 Comparison of measured final displacement-thickness ratio from experiments with predictions by extended mode technique and by "small-deflection" mode technique; illustration for steel plates loaded over central area of radius $a = R/3$.

7 Comparison of measured final displacement-thickness ratio from experiments with predictions by extended mode technique and by "small-deflection" mode technique; illustration for titanium plates loaded over central area of radius $a = R/2$.

8 Comparison of measured final displacement-thickness ratio from experiments with predictions by extended mode technique and by "small-deflection" mode technique; illustration for steel plates loaded over whole plate area. Plates showed radial displacement at edge due to slippage.

9 Profiles of final deflected shape as observed in an experiment and according to extended mode technique; illustration of initial mode shape function.

10 Comparison of response time predicted by extended mode technique with measured times, t_f' at peak displacement, t_f'' at intercept with rising displacement-time curve of line extending final deflection-time curve; illustration for steel plates.

11 Comparison of response time predicted by extended mode technique with measured times, t_f' at peak displacement, t_f'' at intercept with rising displacement-time curve of line extending final deflection-time curve; illustration for titanium plates.

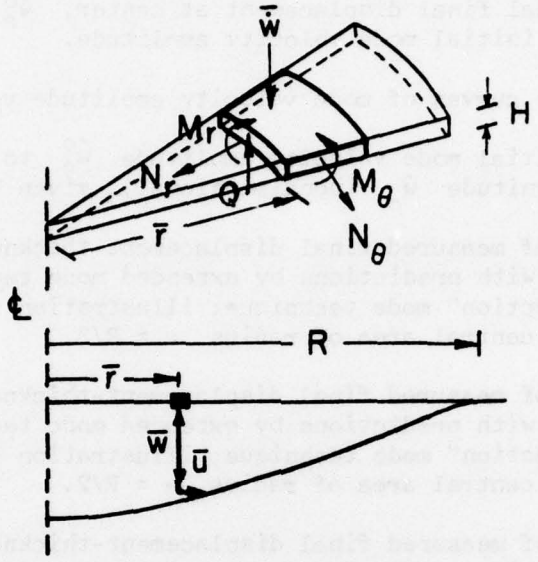

Fig. 1

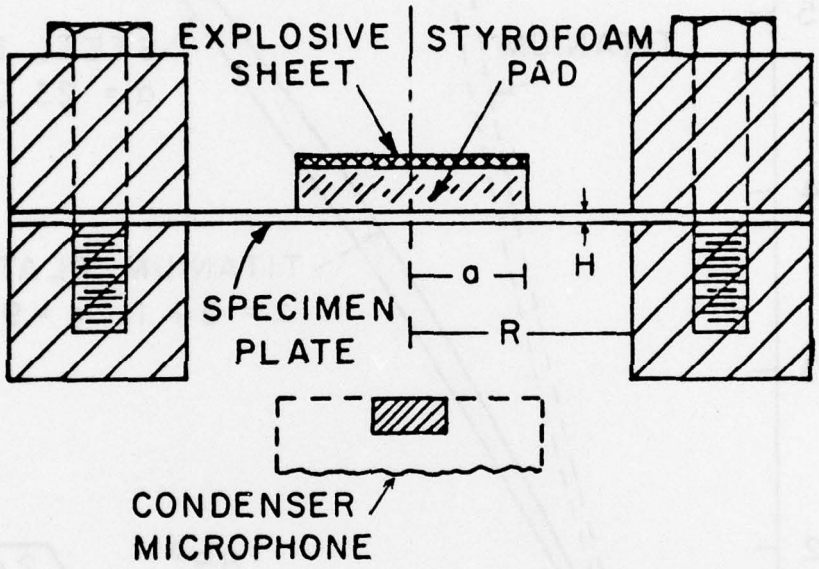
EXPLOSIVE SHEET
STYROFOAM PAD
H
a
R
SPECIMEN PLATE
CONDENSER MICROPHONE

Fig. 2

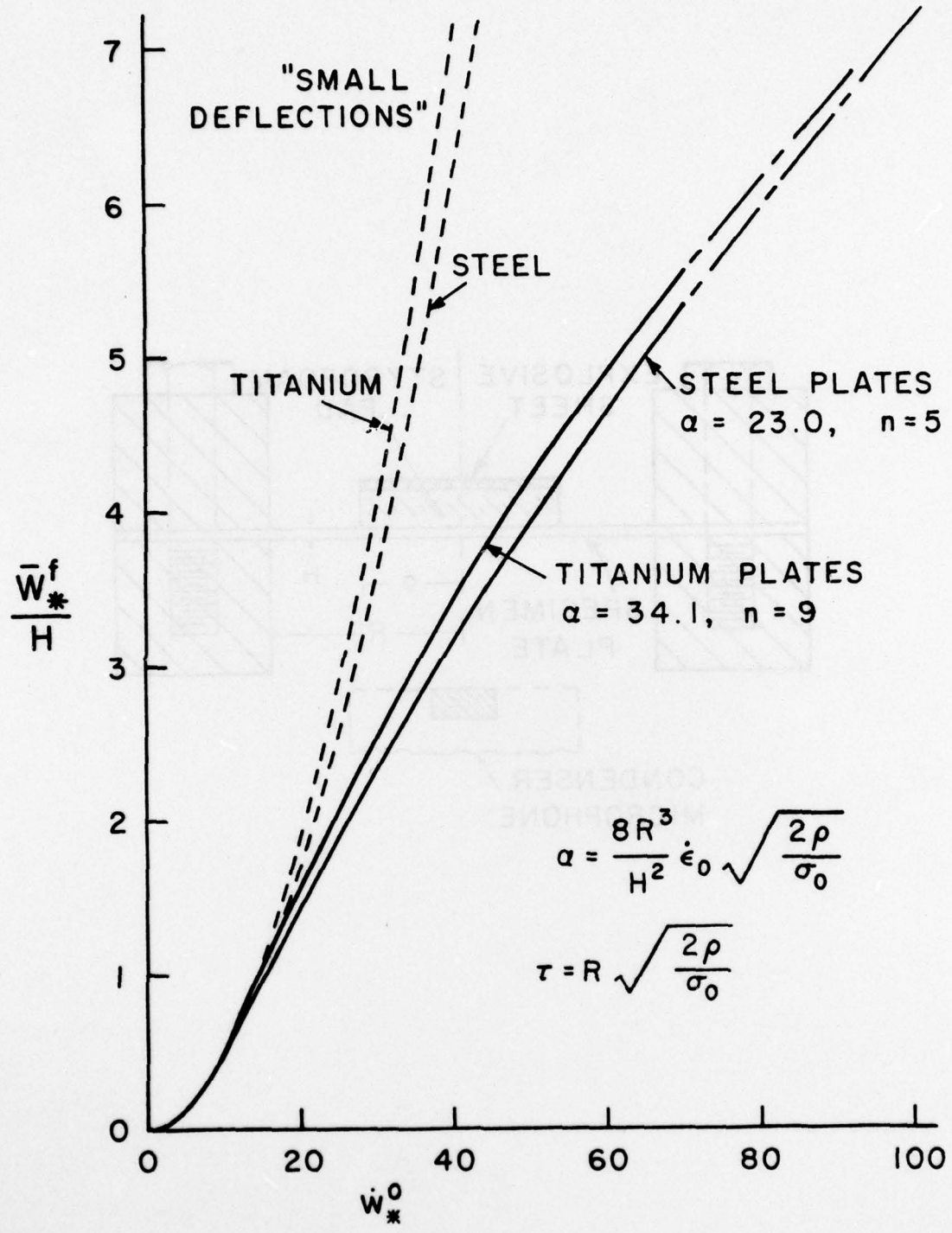
"SMALL DEFLECTIONS"
STEEL
TITANIUM
STEEL PLATES
α = 23.0, n=5
TITANIUM PLATES
α = 34.1, n = 9
$\alpha = \frac{8R^3}{H^2}\dot{\epsilon}_0\sqrt{\frac{2\rho}{\sigma_0}}$
$\tau = R\sqrt{\frac{2\rho}{\sigma_0}}$
$\frac{\bar{W}^f_*}{H}$
$\dot{W}^0_*$
0
1
2
3
4
5
6
7
0
20
40
60
80
100

Fig. 3

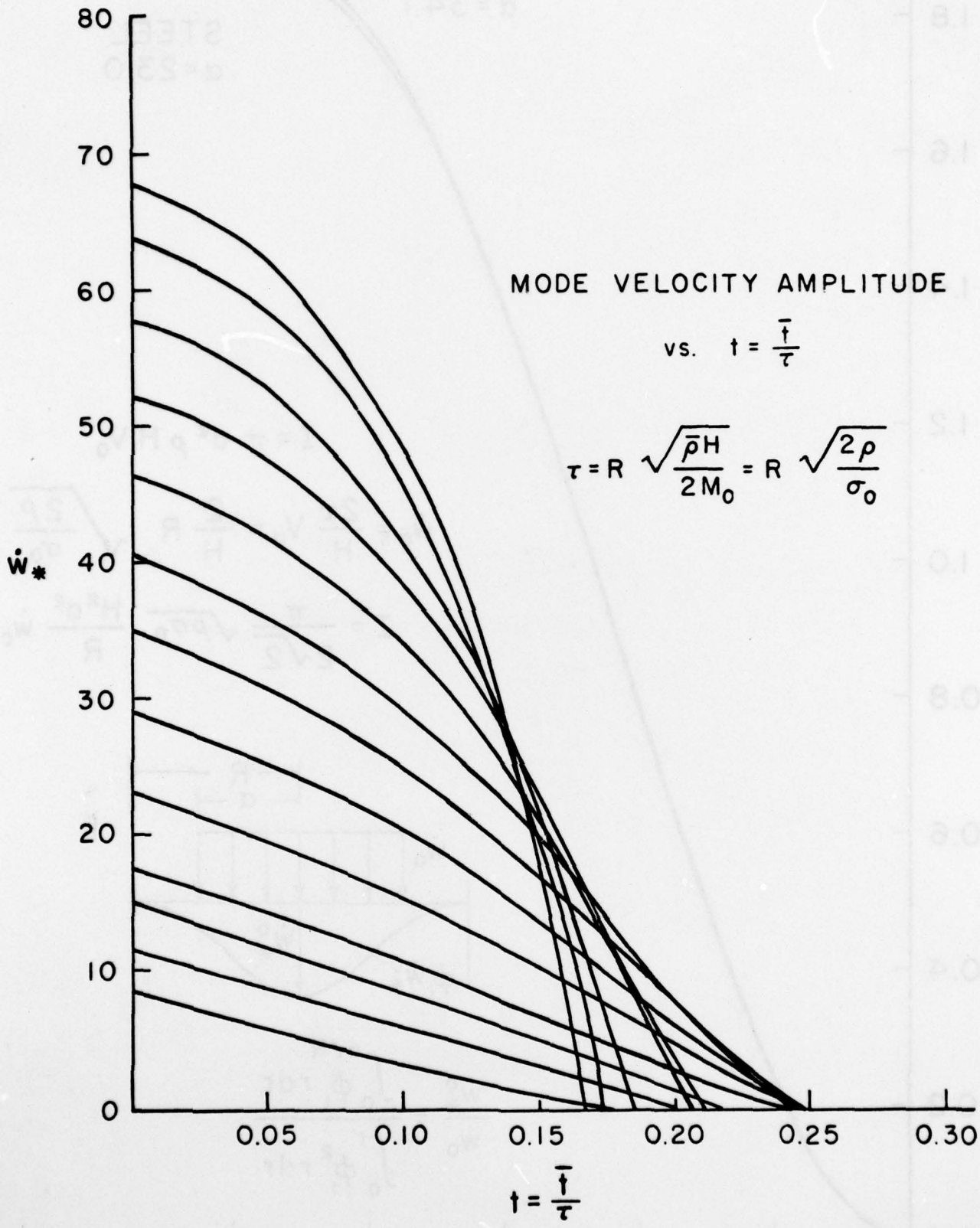
MODE VELOCITY AMPLITUDE
vs. $t = \frac{\bar{t}}{\tau}$
$\tau = R\sqrt{\frac{\bar{\rho}H}{2M_0}} = R\sqrt{\frac{2\rho}{\sigma_0}}$
$\dot{W}_*$
80
70
60
50
40
30
20
10
0
0.05
0.10
0.15
0.20
0.25
0.30
$t = \frac{\bar{t}}{\tau}$

Fig. 4

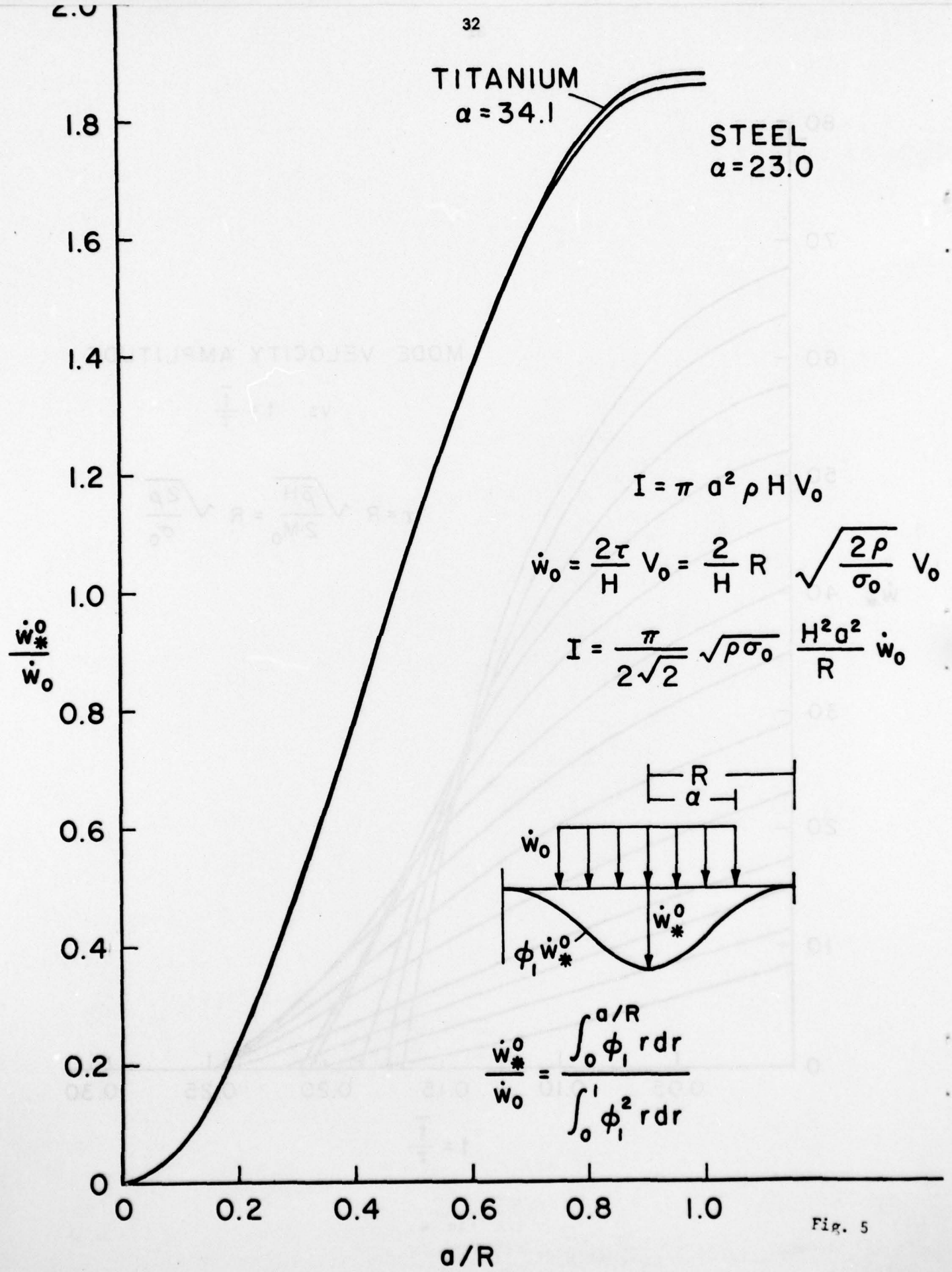
TITANIUM
α = 34.1
STEEL
α = 23.0
$\frac{\dot{w}^0_*}{\dot{w}_0}$
2.0
1.8
1.6
1.4
1.2
1.0
0.8
0.6
0.4
0.2
0
0
0.2
0.4
0.6
0.8
1.0
a/R
$I = \pi a^2 \rho H V_0$
$\dot{w}_0 = \frac{2\tau}{H} V_0 = \frac{2}{H} R \sqrt{\frac{2\rho}{\sigma_0}} V_0$
$I = \frac{\pi}{2\sqrt{2}} \sqrt{\rho\sigma_0} \frac{H^2 a^2}{R} \dot{w}_0$
R
a
$\dot{w}_0$
$\dot{w}^0_*$
$\phi_1 \dot{w}^0_*$
$\frac{\dot{w}^0_*}{\dot{w}_0} = \frac{\int_0^{a/R} \phi_1 \, r dr}{\int_0^1 \phi_1^2 \, r dr}$

Fig. 5

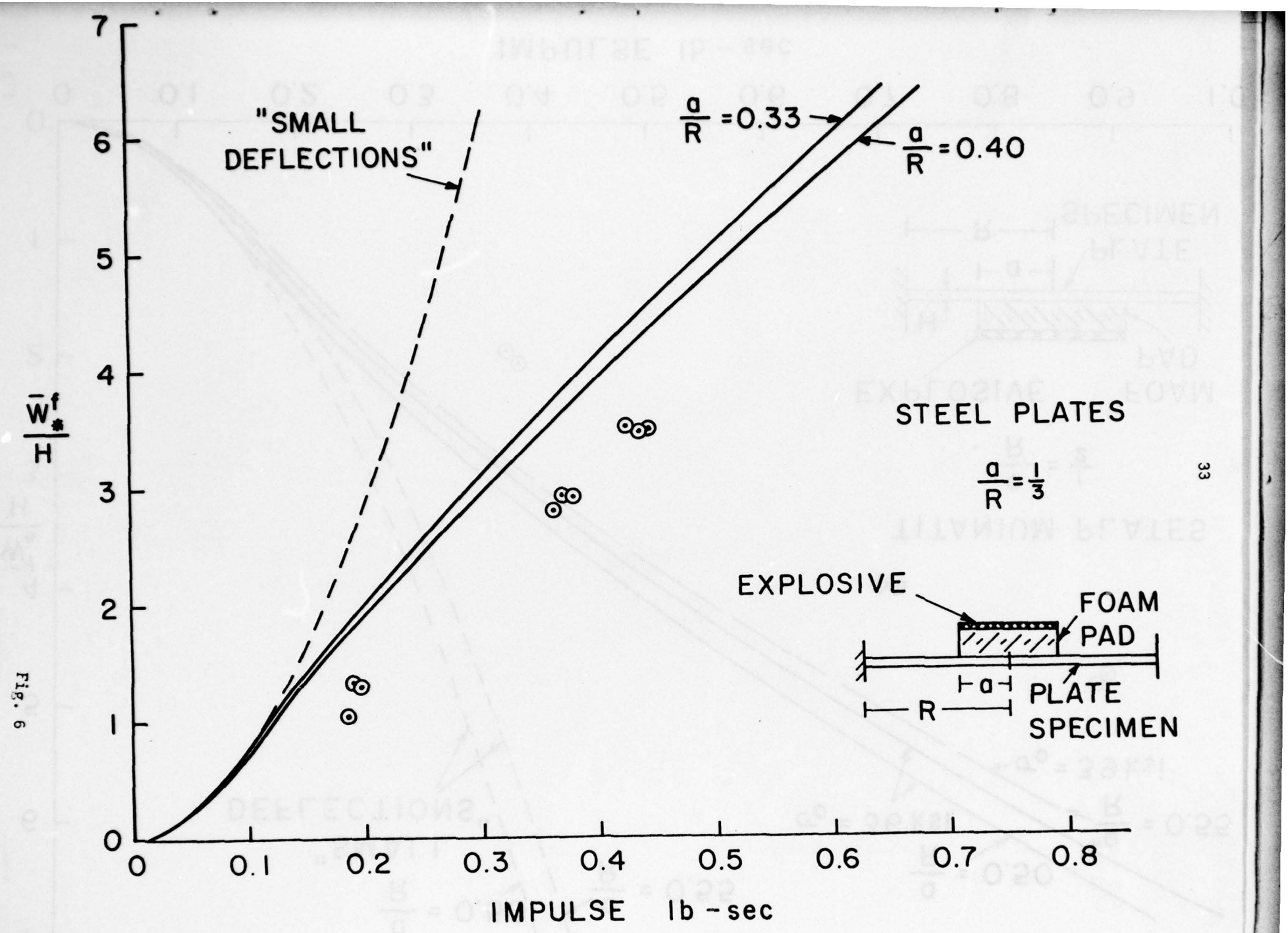
7
6
5
4
3
2
1
0
$\frac{\bar{W}^f_*}{H}$
"SMALL DEFLECTIONS"
$\frac{a}{R}$ =0.33
$\frac{a}{R}$ =0.40
STEEL PLATES
$\frac{a}{R}=\frac{1}{3}$
EXPLOSIVE
FOAM PAD
a
R
PLATE SPECIMEN
0
0.1
0.2
0.3
0.4
0.5
0.6
0.7
0.8
IMPULSE lb-sec

Fig. 6

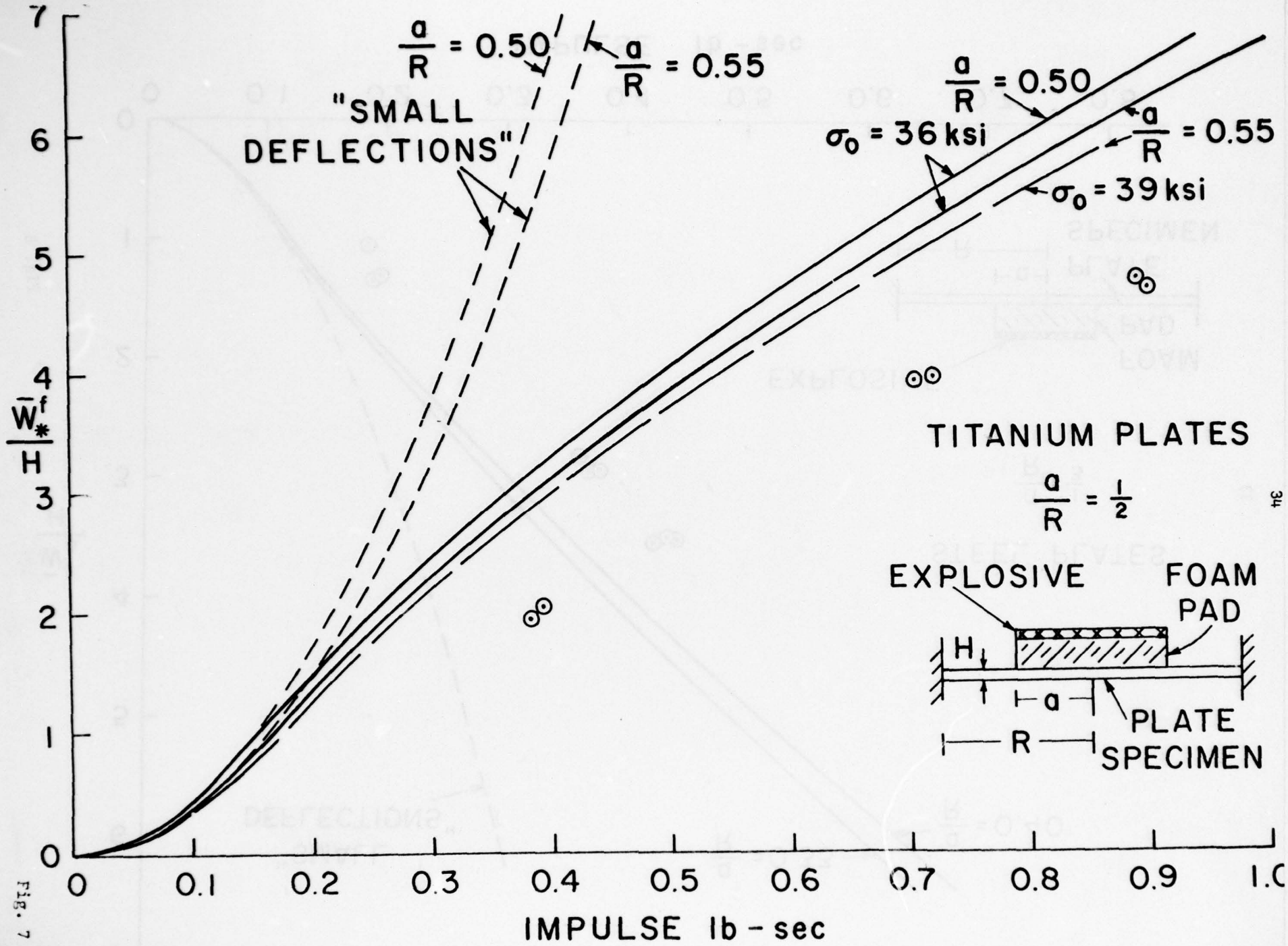
$\frac{a}{R} = 0.50$
$\frac{a}{R} = 0.55$
"SMALL DEFLECTIONS"
$\frac{a}{R} = 0.50$
$\frac{a}{R} = 0.55$
$\sigma_0 = 36$ ksi
$\sigma_0 = 39$ ksi
TITANIUM PLATES
$\frac{a}{R} = \frac{1}{2}$
EXPLOSIVE
FOAM PAD
H
a
R
PLATE SPECIMEN
$\frac{\bar{W}^f_*}{H}$
0
1
2
3
4
5
6
7
0
0.1
0.2
0.3
0.4
0.5
0.6
0.7
0.8
0.9
1.0
IMPULSE lb-sec

Fig. 7

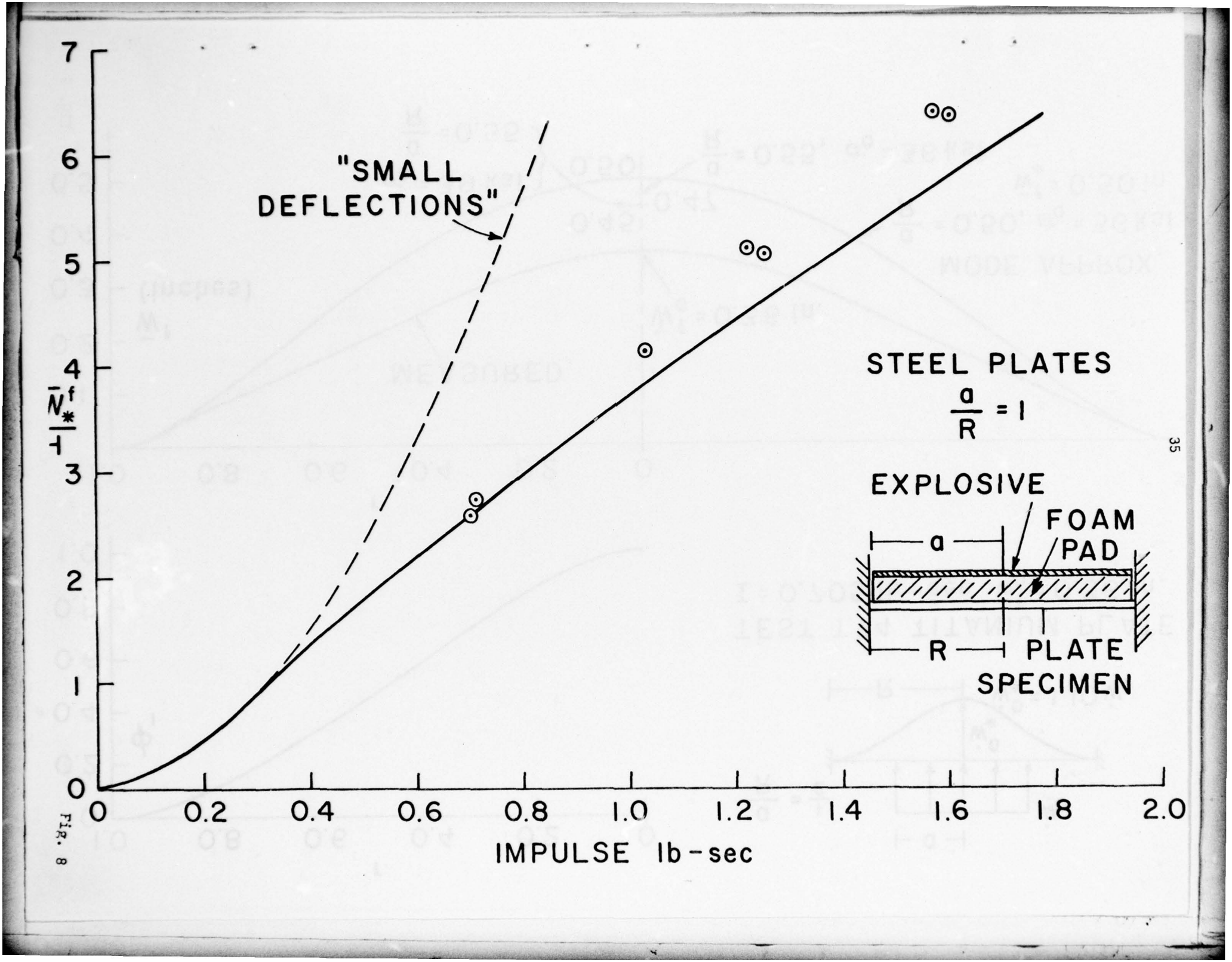
7
6
5
4
3
2
1
0
$\frac{\bar{N}^{f}_{*}}{T}$
"SMALL DEFLECTIONS"
STEEL PLATES
$\frac{a}{R} = 1$
EXPLOSIVE
FOAM PAD
a
R
PLATE SPECIMEN
0
0.2
0.4
0.6
0.8
1.0
1.2
1.4
1.6
1.8
2.0
IMPULSE lb-sec

Fig. 8

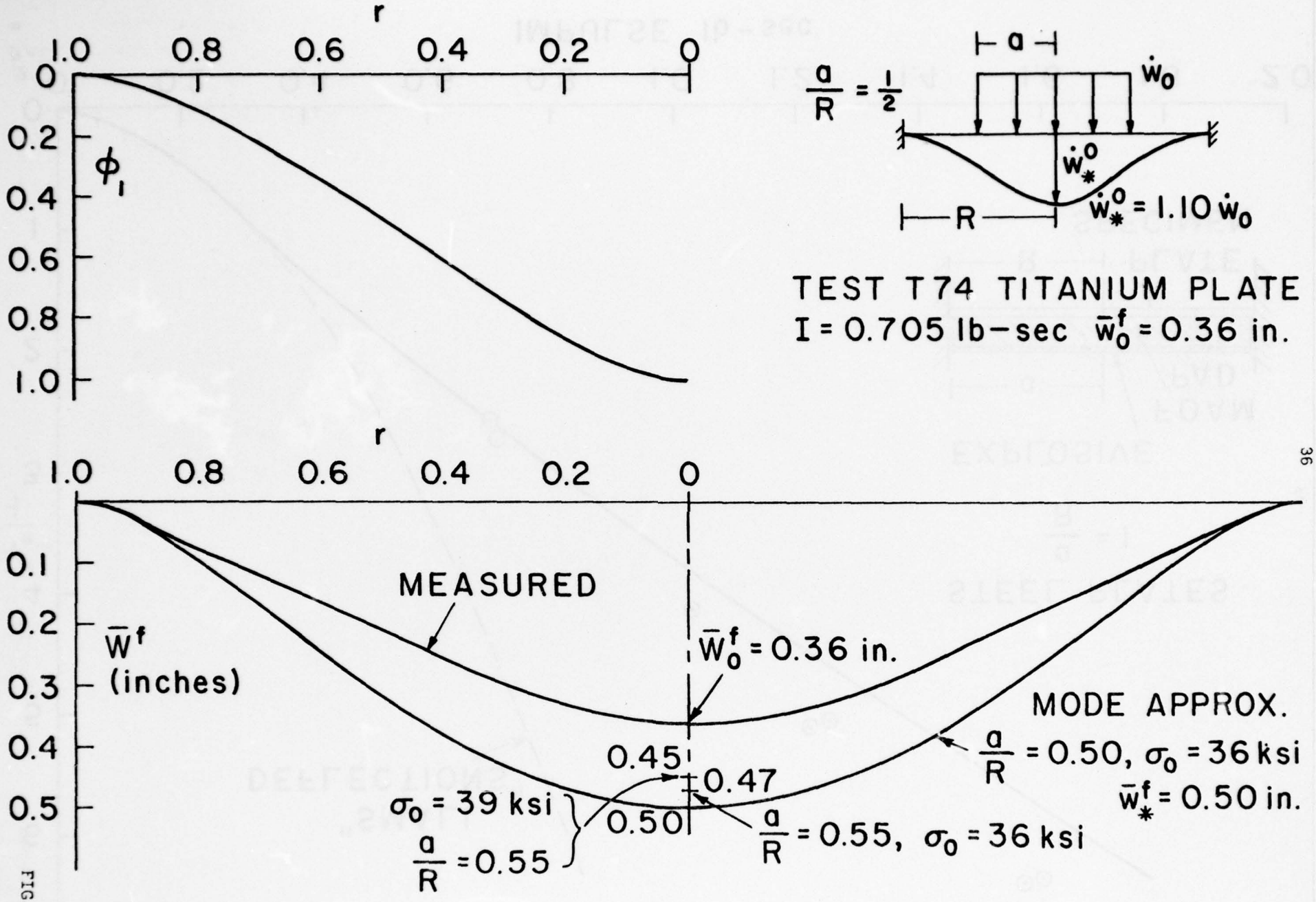
r
1.0
0.8
0.6
0.4
0.2
0
0.2
0.4
0.6
0.8
1.0
ϕ_1
a
$\frac{a}{R} = \frac{1}{2}$
$\dot{w}_0$
$\dot{w}^0_*$
R
$\dot{w}^0_* = 1.10\,\dot{w}_0$
TEST T74 TITANIUM PLATE
I = 0.705 lb-sec $\bar{w}^f_0$ = 0.36 in.
r
1.0
0.8
0.6
0.4
0.2
0
0.1
0.2
0.3
0.4
0.5
$\bar{W}^f$
(inches)
MEASURED
$\bar{W}^f_0$ = 0.36 in.
MODE APPROX.
$\frac{a}{R}$ = 0.50, σ_0 = 36 ksi
$\bar{w}^f_*$ = 0.50 in.
0.45
0.47
0.50
σ_0 = 39 ksi
$\frac{a}{R}$ = 0.55
$\frac{a}{R}$ = 0.55, σ_0 = 36 ksi

FIG. 9

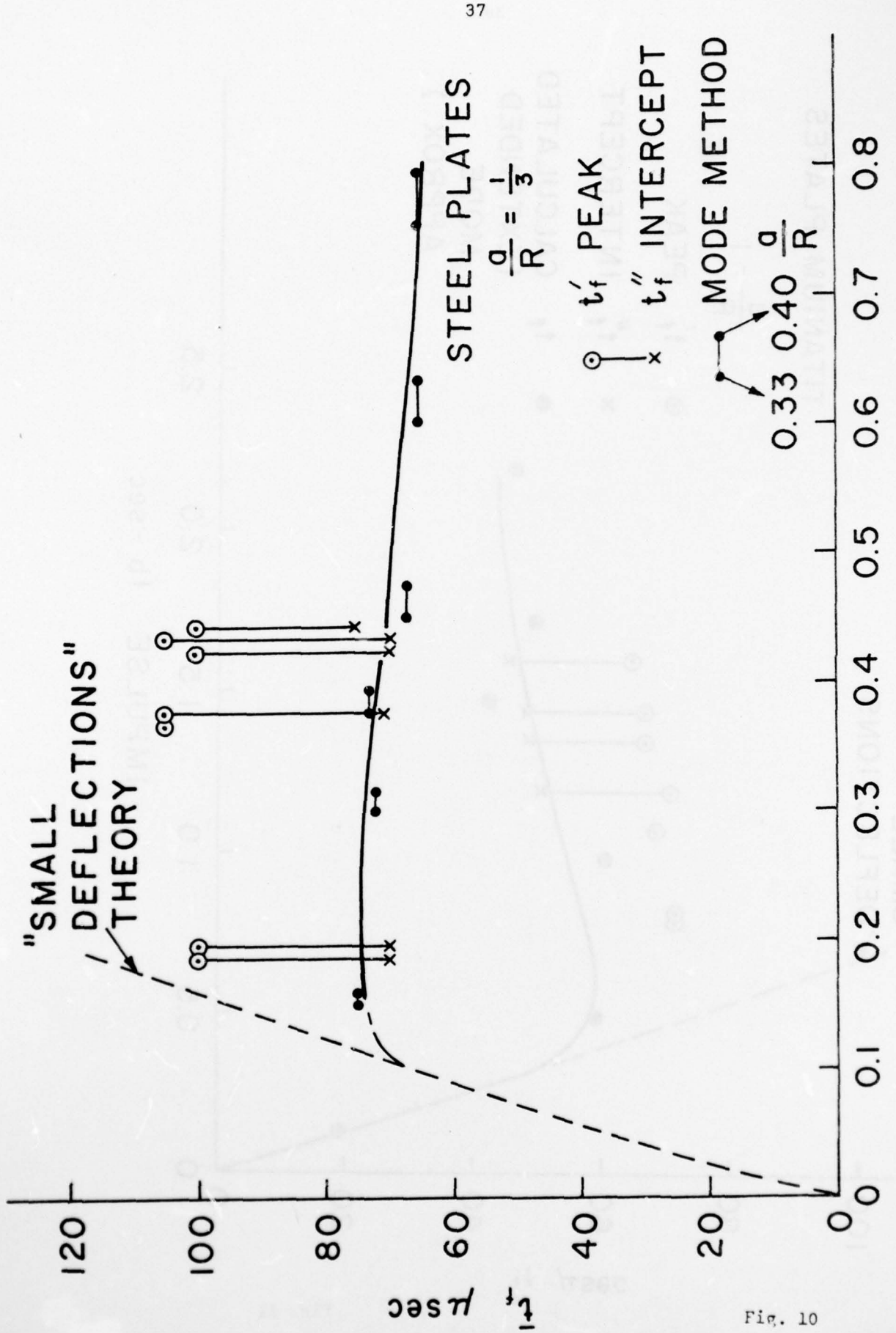
"SMALL DEFLECTIONS" THEORY
STEEL PLATES
$\frac{a}{R} = \frac{1}{3}$
t_f' PEAK
t_f'' INTERCEPT
MODE METHOD
0.33 0.40 $\frac{a}{R}$
t_f μsec
IMPULSE lb - sec
0
20
40
60
80
100
120
0.1
0.2
0.3
0.4
0.5
0.6
0.7
0.8

Fig. 10

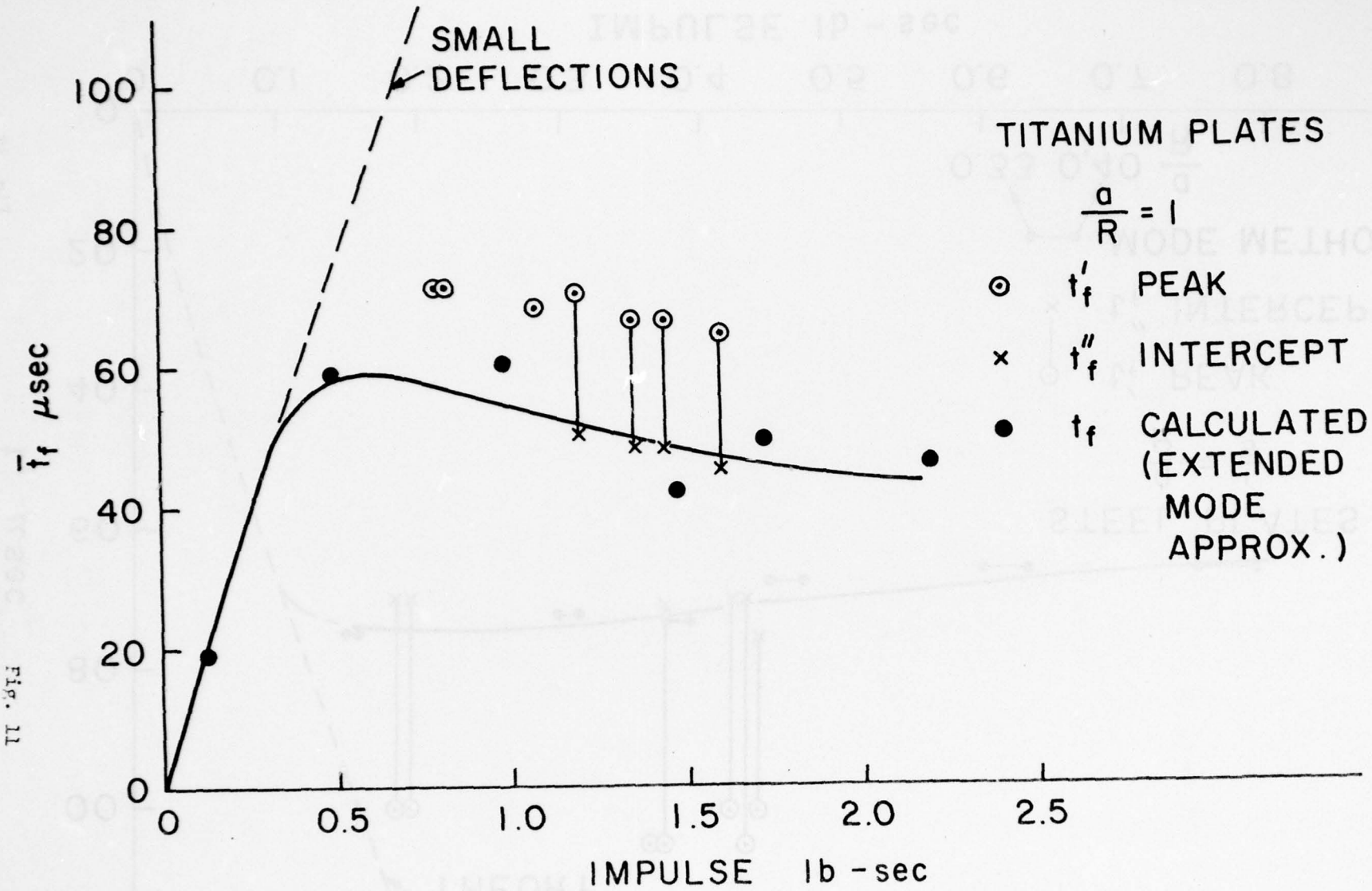
SMALL
DEFLECTIONS
TITANIUM PLATES
$\frac{a}{R} = 1$
t_f' PEAK
t_f'' INTERCEPT
t_f CALCULATED (EXTENDED MODE APPROX.)
$\bar{t}_f$ μsec
100
80
60
40
20
0
0
0.5
1.0
1.5
2.0
2.5
IMPULSE lb-sec

Fig. 11

Security Classification

DOCUMENT CONTROL DATA - R & D

(Security classification of title, body of abstract and indexing annotation must be entered when the overall report is classified)

1. ORIGINATING ACTIVITY (Corporate author)	2a. REPORT SECURITY CLASSIFICATION
Division of Engineering, Brown University Providence, RI 02912	Unclassified
	2b. GROUP

3. REPORT TITLE

Finite Viscoplastic Deflections Of An Impulsively Loaded Plate By The Mode Approximation Technique

4. DESCRIPTIVE NOTES (Type of report and inclusive dates)

Technical Report

5. AUTHOR(S) (First name, middle initial, last name)

Paul S. Symonds
Choon T. Chon

6. REPORT DATE	7a. TOTAL NO. OF PAGES	7b. NO. OF REFS
September 1977	37	17

8a. CONTRACT OR GRANT NO.	9a. ORIGINATOR'S REPORT NUMBER(S)
N00014-75-C-0860 ENG74-21258	N00014 0860/5
b. PROJECT NO.	
c.	9b. OTHER REPORT NO(S) (Any other numbers that may be assigned this report)
d.	

10. DISTRIBUTION STATEMENT

DISTRIBUTION STATEMENT A
Approved for public release;
Distribution Unlimited

11. SUPPLEMENTARY NOTES	12. SPONSORING MILITARY ACTIVITY
	Office of Naval Research

13. ABSTRACT

The application of the mode approximation technique to a fully clamped plate is here described. Mode solutions for finite deflections are obtained from a sequence of instantaneous modes. Master solutions for chosen initial velocity amplitudes are constructed in nondimensional form. These depend weakly on a parameter of viscoplastic material behavior and size of structure, and so can be applied to a variety of loadings and structures. Finding each instantaneous mode shape and acceleration constitutes an eigen-problem, solved by finite elements with iterations. Comparisons with recent tests on steel and titanium plates are discussed in some detail.

DD FORM 1 NOV 68 1473

Security Classification

14. KEY WORDS	LINK A		LINK B		LINK C	
	ROLE	WT	ROLE	WT	ROLE	WT
circular plates						
impulsive						
viscoplastic						
approximation						